EUROPEAN ORGANIZATION FOR NUCLEAR RESEARCH

CERN-PPE/91-43

7 March 1991

A study of the reaction $e^+e^- \to \mu^+\mu^-$ around the Z^0 pole

DELPHI Collaboration

Abstract

Measurements of the cross section and forward-backward asymmetry for the reaction $e^+e^- \to \mu^+\mu^-$ using the DELPHI detector at LEP are presented. The data come from a scan around the Z° peak at seven centre of mass energies, giving a sample of 3858 events in the polar angle region $22^\circ < \theta < 158^\circ$. From a fit to the cross section for $43^\circ < \theta < 137^\circ$, a polar angle region for which the absolute efficiency has been determined, the square root of the product of the $Z^\circ \to e^+e^-$ and $Z^\circ \to \mu^+\mu^-$ partial widths is determined to be $(\Gamma_e\Gamma_\mu)^{1/2} = 85.0 \pm 0.9(\text{stat}) \pm 0.8(\text{syst})$ MeV. From this measurement of the partial width, the value of the effective weak mixing angle is determined to be $\sin^2(\overline{\theta_W}) = 0.2267 \pm 0.0037$. The ratio of the hadronic to muon pair partial widths is found to be $\Gamma_h/\Gamma_\mu = 19.89 \pm 0.40(\text{stat}) \pm 0.19(\text{syst})$. The forward-backward asymmetry at the resonance peak energy $E_{cm*} = 91.22$ GeV is found to be $A_{FB} = 0.028 \pm 0.020(\text{stat}) \pm 0.005(\text{syst})$. From a combined fit to the cross section and forward-backward asymmetry data, the products of the electron and muon vector and axial-vector coupling constants are determined to be $V_eV_\mu = 0.0024 \pm 0.0015(\text{stat}) \pm 0.0004(\text{syst})$ and $A_eA_\mu = 0.253 \pm 0.003(\text{stat}) \pm 0.003(\text{syst})$. These results are in good agreement with the expectations of the Minimal Standard Model.

(Submitted to Physics Letters B)

P.Abreu[16], W.Adam[39], F.Adami[30], T.Adye[29], T.Akesson[19], G.D.Alekseev[12], P.Allen[38], S.Almehed[19], F.Alted[38], S.J.Alvsvaag[4], U.Amaldi[7], E.Anassontzis[3], P.Antilogus[20], W-D.Apel[13], B.Åsman[34], P.Astier[18], J-E.Augustin[15], A.Augustinus[7], P.Baillon[7], P.Bambade[15], F.Barao[16], G.Barbiellini[36], D.Y.Bardin[12], A.Baroncelli[31], O.Barring[19], W.Bartl[39], M.J.Bates[27], M.Baubillier[18], K-H.Becks[41], C.J.Beeston[27], M.Begalli[10], P.Beilliere[6], I.Belokopytov[33], P.Beltran[9], D.Benedic[8], J.M.Benlloch[38], M.Berggren[34], D.Bertrand[2], S.Biagi[17], F.Bianchi[35], J.H.Bibby[27], M.S.Bilenky[12], P.Billoir[18], J.Bjarne[19], D.Bloch[8], P.N.Bogolubov[12], T.Bolognese[30], M.Bonapart[24], M.Bonesini[22], W.Bonivento[22], P.S.L.Booth[17], M.Boratav[18], P.Borgeaud[30], G.Borisov[33], H.Borner[27], C.Bosio[31], O.Botner[37], B.Bouquet[15], M.Bozzo[10], S.Braibant[7], P.Branchini[31], K.D.Brand[28], R.A.Brenner[11], C.Bricman[2], R.C.A.Brown[7], N.Brummer[24], J-M.Brunet[6], L.Bugge[26], T.Buran[26], H.Burmeister[7], J.A.M.A.Buytaert[2], M.Caccia[22], M.Calvi[22], A.J.Camacho Rozas[32], J-E.Campagne[7], A.Campion[17], T.Camporesi[7], V.Canale[31], F.Cao[2], L.Carroll[17], C.Caso[10], E.Castelli[36], M.V.Castillo Gimenez[38], A.Cattai[7], F.R.Cavallo[5], L.Cerrito[31], P.Charpentier[7], P.Checchia[28], G.A.Chelkov[12], L.Chevalier[30], P.Chliapnikov[33], V.Chorowicz[18], R.Cirio[35], M.P.Clara[35], J.L.Contreras[38], R.Contri[10], G.Cosme[15], F.Couchot[15], H.B.Crawley[1], D.Crennell[29], G.Crosetti[10], N.Crosland[27], M.Crozon[6], J.Cuevas Maestro[32], S.Czellar[11], S.Dagoret[15], E.Dahl-Jensen[23], B.Dalmagne[15], M.Dam[7], G.Damgaard[23], G.Darbo[10], E.Daubie[2], P.D.Dauncey[27], M.Davenport[7], P.David[18], A.De Angelis[36], M.De Beer[30], H.De Boeck[2], W.De Boer[13], C.De Clercq[2], M.D.M.De Fez Laso[38], N.De Groot[24], C.De La Vaissiere[18], B.De Lotto[36], C.Defoix[6], D.Delikaris[7], S.Delorme[7], P.Delpierre[6], N.Demaria[35], L.Di Ciaccio[31], H.Dijkstra[7], F.Djama[8], J.Dolbeau[6], M.Donszelmann[24], K.Doroba[40], M.Dracos[7], J.Drees[41], M.Dris[25], W.Dulinski[8], R.Dzhelyadin[33], L-O.Eek[37], P.A.-M.Eerola[11], T.Ekelof[37], G.Ekspong[34], J-P.Engel[8], V.Falaleev[33], D.Fassouliotis[25], A.Fenyuk[33], M.Fernandez Alonso[32], A.Ferrer[38], T.A.Filippas[25], A.Firestone[1], H.Foeth[7], E.Fokitis[25], P.Folegati[36], F.Fontanelli[10], H.Forsbach[41], B.Franek[29], K.E.Fransson[37], P.Frenkiel[6], D.C.Fries[13], A.G.Frodesen[4], R.Fruhwirth[39], F.Fulda-Quenzer[15], K.Furnival[17], H.Furstenau[13], J.Fuster[7], J.M.Gago[16], G.Galeazzi[28], D.Gamba[35], J.Garcia[32], U.Gasparini[28], P.Gavillet[7], E.N.Gazis[25], J-P.Gerber[8], P.Giacomelli[5], K-W.Glitza[41], R.Gokieli[7], V.M.Golovatyuk[12], J.J.Gomez Y Cadenas[7], A.Goobar[34], G.Gopal[29], M.Gorski[40], V.Gracco[10], A.Grant[7], F.Grard[2], E.Graziani[31], M-H.Gros[15], G.Grosdidier[15], B.Grossetete[18], S.Gumenyuk[33], J.Guy[29], F.Hahn[7], M.Hahn[13], S.Haider[24], Z.Hajduk[24], A.Hakansson[19], A.Hallgren[37], K.Hamacher[41], G.Hamel De Monchenault[30], F.J.Harris[27], B.W.Heck[7], I.Herbst[41], J.J.Hernandez[38], P.Herquet[2], H.Herr[7], I.Hietanen[11], E.Higon[38], H.J.Hilke[7], S.D.Hodgson[27], T.Hofmokl[40], R.Holmes[1], S-O.Holmgren[34], D.Holthuizen[24], P.F.Honore[6], J.E.Hooper[23], M.Houlden[17], J.Hrubec[39], P.O.Hulth[34], K.Hultqvist[34], D.Husson[8], B.D.Hyams[7], P.Ioannou[3], D.Isenhower[7], P-S.Iversen[4], J.N.Jackson[17], P.Jalocha[14], G.Jarlskog[19], P.Jarry[30], B.Jean-Marie[15], E.K.Johansson[34], D.Johnson[17], M.Jonker[7], L.Jonsson[19], P.Juillot[8], G.Kalkanis[3], G.Kalmus[29], G.Kantardjian[7], F.Kapusta[18], P.Kapusta[14], S.Katsanevas[3], E.C.Katsoufis[25], R.Keranen[11], J.Kesteman[2], B.A.Khomenko[12], N.N.Khovanski[12], B.King[17], N.J.Kjaer[23], H.Klein[7], W.Klempt[7], A.Klovning[4], P.Kluit[24], J.H.Koehne[13], B.Koene[24], P.Kokkinias[9], M.Kopf[13], M.Koratzinos[7], K.Korcyl[14], A.V.Korytov[12], B.Korzen[7], V.Kostukhin[33], C.Kourkoumelis[3], T.Kreuzberger[39], J.Krolikowski[40], U.Kruener-Marquis[41], W.Krupinski[14], W.Kucewicz[22], K.Kurvinen[11], C.Lambropoulos[9], J.W.Lamsa[1], L.Lanceri[36], V.Lapin[33], J-P.Laugier[30], R.Lauhakangas[11], G.Leder[39], F.Ledroit[6], J.Lemonne[2], G.Lenzen[41], V.Lepeltier[15], A.Letessier-Selvon[18], D.Liko[39], E.Lieb[41], E.Lillethun[4], J.Lindgren[11], A.Lipniacka[40], I.Lippi[28], R.Llosa[38], B.Loerstad[19], M.Lokajicek[12], J.G.Loken[27], M.A.Lopez Aguera[32], A.Lopez-Fernandez[15], M.Los[24], D.Loukas[9], A.Lounis[8], J.J.Lozano[38], R.Lucock[29], P.Lutz[6], L.Lyons[27], G.Maehlum[7], J.Maillard[6], A.Maltezos[9], S.Maltezos[25], F.Mandl[39], J.Marco[32], M.Margoni[28], J-C.Marin[7], A.Markou[9], L.Mathis[6], F.Matorras[32], C.Matteuzzi[22], G.Matthiae[31], M.Mazzucato[28], M.Mc Cubbin[17], R.Mc Kay[1], R.Mc Nulty[17], E.Menichetti[35], C.Meroni[22], W.T.Meyer[1], W.A.Mitaroff[39], G.V.Mitselmakher[12], U.Mjoernmark[19], T.Moa[34], R.Moeller[23], K.Moenig[41], M.R.Monge[10], P.Morettini[10], H.Mueller[13], H.Muller[7], G.Myatt[27], F.Naraghi[18], U.Nau-Korzen[41], F.L.Navarria[5], P.Negri[22], B.S.Nielsen[23], B.Nijjhar[17], V.Nikolaenko[33], V.Obraztsov[33], A.G.Olshevski[12], R.Orava[11], A.Ostankov[33], A.Ouraou[30], R.Pain[18], H.Palka[24], T.Papadopoulou[25], L.Pape[7], A.Passeri[31], M.Pegoraro[28], V.Perevozchikov[33], M.Pernicka[39], A.Perrotta[5], F.Pierre[30], M.Pimenta[16], O.Pingot[2], A.Pinsent[27], M.E.Pol[16], G.Polok[14], P.Poropat[36], P.Privitera[13], A.Pullia[22], J.Pyyhtia[11], D.Radojicic[27], S.Ragazzi[22], W.H.Range[17], P.N.Ratoff[27], A.L.Read[26], N.G.Redaelli[22], M.Regler[39], D.Reid[17], P.B.Renton[27], L.K.Resvanis[3], F.Richard[15], M.Richardson[17], J.Ridky[12], G.Rinaudo[35], I.Roditi[7], A.Romero[35], P.Ronchese[28], C.Ronnqvist[11], E.I.Rosenberg[1], U.Rossi[5], E.Rosso[7], P.Roudeau[15], T.Rovelli[5], W.Ruckstuhl[24], V.Ruhlmann[30], A.Ruiz[32], K.Rybicki[14], H.Saarikko[11], Y.Sacquin[30], J.Salt[38], E.Sanchez[38], J.Sanchez[38], M.Sannino[10], M.Schaeffer[8], H.Schneider[13], F.Scuri[36], A.M.Segar[27], R.Sekulin[29], M.Sessa[36], G.Sette[10], R.Seufert[13], R.C.Shellard[16],

P.Siegrist[30], S.Simonetti[10], F.Simonetto[28], A.N.Sissakian[12], T.B.Skaali[26], G.Skjevling[26], G.Smadja[20], G.R.Smith[29], R.Sosnowski[40], T.S.Spassoff[12], E.Spiriti[31], S.Squarcia[10], H.Staeck[41], C.Stanescu[31], G.Stavropoulos[9], F.Stichelbaut[2], A.Stocchi[22], J.Strauss[39], R.Strub[8], C.J.Stubenrauch[7], M.Szczekowski[40], M.Szeptycka[40], P.Szymanski[40], S.Tavernier[2], G.Theodosiou[9], A.Tilquin[21], J.Timmermans[24], V.G.Timofeev[12], L.G.Tkatchev[12], T.Todorov[12], D.Z.Toet[24], L.Tortora[31], M.T.Trainor[27], D.Treille[7], U.Trevisan[10], W.Trischuk[7], G.Tristram[6], C.Troncon[22], A.Tsirou[7], E.N.Tsyganov[12], M.Turala[14], R.Turchetta[8], M-L.Turluer[30], T.Tuuva[11], I.A.Tyapkin[12], M.Tyndel[29], S.Tzamarias[7], S.Ueberschaer[41], O.Ullaland[7], V.A.Uvarov[33], G.Valenti[5], E.Vallazza[35], J.A.Valls Ferrer[38], G.W.Van Apeldoorn[24], P.Van Dam[24], W.K.Van Doninck[2], N.Van Eijndhoven[7], C.Vander Velde[2], J.Varela[16], P.Vaz[16], G.Vegni[22], J.Velasco[38], L.Ventura[28], W.Venus[29], F.Verbeure[2], L.S.Vertogradov[12], L.Vibert[18], D.Vilanova[30], E.V.Vlasov[33], A.S.Vodopyanov[12], M.Vollmer[41], S.Volponi[5], G.Voulgaris[3], M.Voutilainen[11], V.Vrba[31], H.Wahlen[41], C.Walck[34], F.Waldner[36], M.Wayne[1], P.Weilhammer[7], J.Werner[41], A.M.Wetherell[7], J.H.Wickens[2], J.Wikne[26], G.R.Wilkinson[27], W.S.C.Williams[27], M.Winter[8], D.Wormald[26], G.Wormser[15], K.Woschnagg[37], N.Yamdagni[34], P.Yepes[7], A.Zaitsev[33], A.Zalewska[14], P.Zalewski[40], E.Zevgolatakos[9], G.Zhang[41], N.I.Zimin[12], M.Zito[30], R.Zitoun[18], R.Zukanovich Funchal[6], G.Zumerle[28], J.Zuniga[38]

[1]Ames Laboratory and Department of Physics, Iowa State University, Ames IA 50011, USA
[2]Physics Department, Univ. Instelling Antwerpen, Universiteitsplein 1, B-2610 Wilrijk, Belgium
and IIHE, ULB-VUB, Pleinlaan 2, B-1050 Brussels, Belgium
and Service de Phys. des Part. Elém., Faculté des Sciences, Université de l'Etat Mons, Av. Maistriau 19, B-7000 Mons, Belgium
[3]Physics Laboratory, University of Athens, Solonos Str. 104, GR-10680 Athens, Greece
[4]Department of Physics, University of Bergen, Allégaten 55, N-5007 Bergen, Norway
[5]Dipartimento di Fisica, Università di Bologna and INFN, Via Irnerio 46, I-40126 Bologna, Italy
[6]Collège de France, Lab. de Physique Corpusculaire, 11 pl. M. Berthelot, F-75231 Paris Cedex 05, France
[7]CERN, CH-1211 Geneva 23, Switzerland
[8]Division des Hautes Energies, CRN - Groupe DELPHI and LEPSI, B.P.20 CRO, F-67037 Strasbourg Cedex, France
[9]Institute of Nuclear Physics, N.R.C. Demokritos, P.O. Box 60628, GR-15310
Athens, Greece
[10]Dipartimento di Fisica, Università di Genova and INFN, Via Dodecaneso 33, I-16146 Genova, Italy
[11]Research Institute for High Energy Physics, University of Helsinki, Siltavuorenpenger 20 C, SF-00170 Helsinki 17, Finland
[12]Joint Institute for Nuclear Research, Dubna, Head Post Office, P.O. Box 79, 101 000 Moscow, USSR.
[13]Institut für Experimentelle Kernphysik, Universität Karlsruhe, Postfach 6980, D-7500 Karlsruhe 1, FRG
[14]High Energy Physics Laboratory, Institute of Nuclear Physics, Ul. Kawiory 26 a, PL-30055 Krakow 30, Poland
[15]Université de Paris-Sud, Lab. de l'Accélérateur Linéaire, Bat 200, F-91405 Orsay, France
[16]LIP, Av. Elias Garcia 14 - 1e, P-1000 Lisbon Codex, Portugal
[17]Department of Physics, University of Liverpool, P.O. Box 147, GB - Liverpool L69 3BX, UK
[18]LPNHE, Universités Paris VI et VII, Tour 33 (RdC), 4 place Jussieu, F-75230 Paris Cedex 05, France
[19]Department of Physics, University of Lund, Sölvegatan 14, S-22363 Lund, Sweden
[20]Université Claude Bernard de Lyon, 43 Bd du 11 Novembre 1918, F-69622 Villeurbanne Cedex, France
[21]Faculté des Sciences de Luminy, 163 Avenue de Luminy, case 907, F-13288 Marseille Cedex 09, France
[22]Dipartimento di Fisica, Università di Milano and INFN, Via Celoria 16, I-20133 Milan, Italy
[23]Niels Bohr Institute, Blegdamsvej 17, DK-2100 Copenhagen 0, Denmark
[24]NIKHEF-H, Postbus 41882, NL-1009 DB Amsterdam, The Netherlands
[25]National Technical University, Physics Department, Zografou Campus, GR-15773 Athens, Greece
[26]Physics Department, University of Oslo, Blindern, N-1000 Oslo 3, Norway
[27]Nuclear Physics Laboratory, University of Oxford, Keble Road, GB - Oxford OX1 3RH, UK
[28]Dipartimento di Fisica, Università di Padova and INFN, Via Marzolo 8, I-35131 Padua, Italy
[29]Rutherford Appleton Laboratory, Chilton, GB - Didcot OX11 OQX, UK
[30]CEN-Saclay, DPhPE, F-91191 Gif-sur-Yvette Cedex, France
[31]Istituto Superiore di Sanità, Ist. Naz. di Fisica Nucl. (INFN), Viale Regina Elena 299, I-00161 Rome, Italy
and Dipartimento di Fisica, Università di Roma II and INFN, Tor Vergata, I-00173 Rome.
[32]Facultad de Ciencias, Universidad de Santander, av. de los Castros, E - 39005 Santander, Spain
[33]Inst. for High Energy Physics, Serpukow P.O. Box 35, Protvino, (Moscow Region), USSR.
[34]Institute of Physics, University of Stockholm, Vanadisvägen 9, S-113 46 Stockholm, Sweden
[35]Dipartimento di Fisica Sperimentale, Università di Torino and INFN, Via P. Giuria 1, I-10125 Turin, Italy
[36]Dipartimento di Fisica, Università di Trieste and INFN, Via A. Valerio 2, I-34127 Trieste, Italy
and Istituto di Fisica, Università di Udine, I-33100 Udine, Italy
[37]Department of Radiation Sciences, University of Uppsala, P.O. Box 535, S-751 21 Uppsala, Sweden
[38]Inst. de Fisica Corpuscular IFIC, Centro Mixto Univ. de Valencia-CSIC, Avda. Dr. Moliner 50, E-46100 Burjassot (Valencia), Spain
[39]Institut für Hochenergiephysik, Österreich Akad. d. Wissensch., Nikolsdorfergasse 18, A-1050 Vienna, Austria
[40]Inst. Nuclear Studies and, University of Warsaw, Ul. Hoza 69, PL-00681 Warsaw, Poland
[41]Fachbereich Physik, University of Wuppertal, Postfach 100 127, D-5600 Wuppertal 1, FRG

1. Introduction

A study of the reaction $e^+e^- \rightarrow \mu^+\mu^-$ at energies around the Z° pole can provide one of the cleanest tests available of the Standard Model [1]. Precise calculations of both the cross section and the forward-backward asymmetry can be made, including the effects of realistic experimental cuts [2]. These calculations include higher order electromagnetic and weak effects, and are not subject to assumptions about the final state electromagnetic radiation from quarks and/or hadrons, as is the case in the hadronic final states. Furthermore, the theoretical interpretation is free of uncertainties arising from final state QCD and hadronisation corrections. Experimentally the $\mu^+\mu^-$ final state is distinctive and can be extracted cleanly from background processes.

In this paper results are presented on the cross section

$$\sigma_{\mu\mu}(E_{cms}) = \sigma(e^+e^- \rightarrow \mu^+\mu^-),$$

where E_{cms} $(= \sqrt{s})$ is the e^+e^- centre of mass energy, and on the forward-backward asymmetry

$$A_{FB}(E_{cms}) = \frac{\sigma^F_{\mu\mu} - \sigma^B_{\mu\mu}}{\sigma^F_{\mu\mu} + \sigma^B_{\mu\mu}}.$$

In this expression, $\sigma^F_{\mu\mu}(\sigma^B_{\mu\mu})$ is the cross section for the production of a μ^- with $\cos\theta > 0 (< 0)$, where θ is the angle of the μ^- with respect to the incident e^- direction. The results of a previous study of $\sigma_{\mu\mu}$ as a function of E_{cms}, from data taken in 1989, can be found in reference [3]. Results on this subject from the other experiments at similar energies can be found in reference [4].

2. Apparatus and data collection

Results are presented on data taken using the DELPHI detector at the LEP e^+e^- collider at CERN during 1990 at seven centre of mass energies. The values of $\sqrt{s}$ used are those computed taking into account the results of the LEP beam energy calibration measurements [5]. The uncertainty on $\sqrt{s}$ from the LEP measurements is ± 0.02 GeV.

Details of the DELPHI detector can be found in reference [6]. The analysis procedure for the selection of candidate $e^+e^- \rightarrow \mu^+\mu^-$ events in the barrel region is similar to that presented in reference [3]. In this analysis the polar angle range for the determination of cross sections has been increased to $43^\circ < \theta < 137^\circ$. For the determination of the forward-backward asymmetry the polar angle range has been further extended to $22^\circ < \theta < 158^\circ$. This larger angular acceptance for the asymmetry measurements is important as the size of the error is related to the maximum absolute value of $\cos\theta$ in the data sample.

Track reconstruction was performed using the time projection chamber (TPC), complemented by the inner (ID) and outer (OD) tracking detectors as well as chambers FCA and FCB in the forward region [6]. It was required that there were two tracks, one having a momentum greater than 20 GeV/c and the second having a momentum greater than 15 GeV/c, both coming from the interaction region. This region is defined by $|\delta z| < 4.5$ cm and $\delta r < 1.5$ cm, where δz and δr are the distances of closest approach to the nominal interaction point in the longitudinal and radial directions respectively. The acollinearity angle between the two tracks was required to be less than 10°. It was further required that there were no additional charged particles with momenta greater

than 5 GeV/c. The momentum resolution on the reconstructed tracks used in this analysis can be seen in the distribution of the electric charge multiplied by the inverse of the momentum (Fig.1). This figure also demonstrates that the sign of the electric charge of the muons can be measured reliably, thus making possible a determination of the forward-backward asymmetry. The momentum resolution σ_p/p for the tracks in the barrel region (i.e. TPC plus ID and OD) is 0.08, for tracks having a momentum of about 45 GeV. The corresponding resolution for tracks in the forward region (i.e. TPC plus ID, FCA and FCB) is 0.12.

Three sub-detectors were used in the muon identification in the barrel region. For the barrel muon chambers (MUB), identification was based on the association of the positions of the MUB hits with those expected from the extrapolation of the tracks. For the hadron calorimeter (HCAL), it was required that the energy deposited was consistent with that expected for a minimum ionising particle; namely that the total energy deposited was less than a cut-off value (which was 10 GeV at $\theta = 90°$ and increasing to about 15 GeV at $\theta = 55°$, and thereafter independent of θ) and that there were energy deposits in at least two of the four layers. For the barrel electromagnetic calorimeter (the high density projection chamber, HPC) it was required that there were energy depositions and that these were consistent with those expected from a minimum ionising particle (i.e. less than 1 GeV within $\pm 5°$ in theta and $\pm 10°$ in azimuth around the track extrapolated to the entry point of the HPC). It was required that each particle was identified as a muon by at least one of the three sub-detectors mentioned above in either the barrel or forward regions. Events in which one or both particles was identified as a hadron by HCAL (deposited energy greater than the above cut-off value) or in which both particles were associated with energy deposits greater than 10 GeV in the HPC, and which had an acollinearity angle greater than 1° were removed. The cosmic ray background was almost entirely removed by timing measurements using both the time of flight detector (TOF) and the OD. In the forward region, the identification procedure was similar to that in the barrel, utilizing the forward muon chambers (MUF), the forward part of the hadron calorimeter and the forward electromagnetic calorimeter (FEMC), for which an energy cut-off value of 3 GeV for a minimum ionising particle was used.

The identification efficiency of each of the sub-detectors was measured from the data itself, by counting the number of muon-pairs found by a given sub-detector in a sample defined by the other two sub-detectors. The identification efficiencies were measured as a function of θ. From these studies it was found that the overall muon identification efficiency, which is the 'or' of the three sub-detector efficiencies, was 0.995 ± 0.002 over the θ range $43° < \theta < 137°$. A more restrictive cut on the acollinearity angle was made for the determination of the muon identification efficiency, in order to minimise the effect of the τ-background.

The detection efficiencies and the validity of the method of the efficiency determination were cross-checked by generating a sample of $\mu^+\mu^-$ events using the DYMU3 generator [7] and passing the simulated raw data from the DELPHI detector simulation program [8] through the same analysis chain as for the real data. Simulated events for the $\tau^+\tau^-$ final state, produced using the KORALZ generator [9], were also analysed for background studies.

3. Cross section for $e^+e^- \to \mu^+\mu^-$

The cross section for $e^+e^- \to \mu^+\mu^-$ has been determined for the sample of events in which at least one muon was in the polar angle region $43° < \theta < 137°$. It was required that all the sub-detector components used in the analysis were fully operational. The number of muon-pair events in this sample is 2475. The total integrated luminosity used for the determination of the cross section is 3.9 pb^{-1}, corresponding to about 81,000 hadronic $Z°$ events.

In order to determine the cross section $\sigma_{\mu\mu}$ the number of events at each energy was corrected for the efficiency of muon identification and by the following factors:

- 1.067 ± 0.005, for loss of tracks, mostly from the dead space of the TPC. The error on this correction includes that arising from imprecision on the cuts on momenta and on the polar angle θ.
- 1.019 ± 0.003 for trigger efficiency; this was determined by comparing which triggers fired, on an event by event basis, from a redundant set of triggers based on the ID, TPC and OD track detectors and the TOF detector.
- 0.990 ± 0.005, for the $\tau^+\tau^-$ background; this was estimated from Monte Carlo simulations as described above.
- 0.994 ± 0.002, for the residual cosmic ray background.

The background from the process $e^+e^- \to e^+e^-\mu^+\mu^-$, where the final state e^+ and e^- remain undetected, has been estimated using the event generator described in reference [10]. This background, together with that from $e^+e^- \to e^+e^-$, is found to be negligible.

The luminosity was determined by using the cross section for the Bhabha scattering process $e^+e^- \to e^+e^-$ at small angles and determining the number of these events in a precisely defined angular region, as described in reference [11]. The estimated experimental systematic error on the luminosity for this data sample is 0.8%. Combining this with the estimated theoretical uncertainty of 0.5% gives a total systematic error on the luminosity of 0.9%, which reflects an improved understanding of the sources of theoretical uncertainty in the small angle Bhabha cross section [11].

The cross section for $e^+e^- \to \mu^+\mu^-$, as a function of the centre of mass energy is given in Table 1. The results are corrected for the cuts on momenta, acollinearity and polar angles, and correspond to the full 4π angular acceptance. The correction factors are computed using the formulae of reference [2]. The estimated uncertainty on this calculation is $\pm 0.2\%$, and this is added quadratically to the above errors to give a total systematic error on the cross section of 0.8%, in addition to the error on the luminosity. The results are also displayed in Fig.2a, along with the result of a fit to the data using the program ZFITTER [12]. This program allows a precise calculation of the cross section in terms of the mass M_Z and width Γ_Z of the $Z°$ as well as the leptonic partial widths Γ_ℓ ($\ell = e, \mu$). Fixing the mass and total width of the $Z°$ to be $M_Z = 91.181$ GeV and $\Gamma_Z = 2.455$ GeV, as determined from an analysis of the hadronic line-shape for the data given in reference [11], the fit gives

$$(\Gamma_e\Gamma_\mu)^{1/2} = 85.0 \pm 0.9(\text{stat}) \pm 0.8(\text{syst}) \text{ MeV},$$

with a χ^2/d.o.f. of $8.1/(7-1)$, and where the systematic error includes a contribution of 0.6 MeV from the estimated uncertainty on $\Gamma_Z(\pm 0.020$ GeV) and on $M_Z(\pm 0.022$ GeV), together with the systematic errors quoted above. The component of the above

systematic error arising from the theoretical uncertainty on the Bhabha cross section in the determination of the luminosity is 0.2 MeV. The result for $(\Gamma_e\Gamma_\mu)^{1/2}$ is in good agreement with that of the previous analysis [3], based on a much smaller event sample.

In the Minimal Standard Model the leptonic partial width can be expressed in terms of an effective weak mixing angle $\sin^2(\overline{\theta_W})$ [13]. Combining the statistical and sytematic errors in quadrature gives $\Gamma_l = 85.0 \pm 1.2$ MeV from which we obtain:

$$\sin^2(\overline{\theta_W}) = 0.2267 \pm 0.0037.$$

The ratio of the muon-pair to hadronic cross sections has also been determined. The selection procedure and correction factors of the hadronic events are similar to those described in reference [11]. This quantity is free of uncertainties in the luminosity. Combining the results for all beam energies, and correcting this ratio for the effects of the s-channel photon contribution, gives the following ratio for the partial widths

$$\Gamma_h/\Gamma_\mu = 19.89 \pm 0.40(\text{stat}) \pm 0.19(\text{syst}).$$

In the Minimal Standard Model the value of Γ_ℓ depends on the top quark mass m_t and the mass of the neutral Higgs scalar m_H. For $50 \leq m_t \leq 230$ GeV and $40 \leq m_H \leq 1000$ GeV the expected values for Γ_ℓ are in the range 83.0 to 84.9 MeV (with the variation coming primarily from m_t). The ratio of hadronic to muon pair partial widths is rather insensitive to the variation of the top quark and Higgs boson masses. However, this ratio does depend on the value of the strong coupling constant α_s. Taking $\alpha_s = 0.110 \pm 0.003(stat) \pm 0.003$ (*scale error*), as determined by the DELPHI experiment [14], the Minimal Standard Model predicts a value of 20.69 ± 0.05.

A combined fit to the muon and hadron cross section data has been made with the top-quark mass as a free parameter. The values of M_Z,m_H and α_s were allowed to vary within the ranges quoted above. Within the context of the Minimal Standard Model the top-quark mass is found to be less than 200 GeV at the 95 % confidence level.

4. Forward-backward asymmetry

For this analysis it was required that there was at least one muon in the polar angle region $22° < \theta < 158°$. The absolute detection efficiency has not yet been determined for the extended parts of this polar angle region, however only the relative detection efficiency as a function of angle is required for this analysis, and the inclusion of this region increases the precision significantly. The other selection criteria are the same as those described above, except that a less restrictive set of data taking runs was used since an absolute normalisation is not required. The resulting sample contained 3858 events. In this sample there are 87(27) apparently like-sign muon-pair events (56(11) positive pairs and 31(16) negative pairs), where the numbers in parentheses are for the restricted angular region $43° < \theta < 137°$. For these events the charge assignment was based on the charge of the particle with the smaller momentum error. The relative muon detection efficiency $\epsilon_\mu(|\cos\theta|)$ was determined by comparing the number of events found as a function of $|\cos\theta|$ with the distribution $(1 + \cos^2\theta)$. This function was then used to compute the factor by which the measured value of the forward-backward asymmetry should be corrected for inefficiencies and to correspond to the full (4π) angular range. The resulting values, as a function of E_{cms}, are given

in Table 2 and shown in Fig.2b. The errors shown are statistical only. The values of A_{FB} are not corrected for the momenta and acollinearity cuts.

Possible systematic uncertainties on A_{FB} can arise from several sources: the wrong assignments of the charges of the particles; differences in the detection efficiencies of positive and negative particles in the forward and backward hemispheres; or in systematic differences in the momentum or polar angle values determined for positive and negative tracks in the forward and backward hemispheres. From a series of studies into the above effects, the systematic error on the asymmetry is estimated to be 0.5%.

For the peak cross section point, $E_{cms} = 91.22$ GeV, the value obtained is

$$A_{FB}^{peak} = 0.028 \pm 0.020(\text{stat}) \pm 0.005(\text{syst}).$$

The change in sign of A_{FB}, from negative below the Z° pole to positive above it, arises from a change in sign of the interference term of the photon and Z° exchange diagrams in passing through the pole. Also shown in Fig.2 are the results of a combined fit to A_{FB} and the cross section data $\sigma_{\mu\mu}$ (the curves overlaying the cross section points in this fit and the previous one are indistinguishable). In this fit M_Z and Γ_Z were fixed at the values given above and the fit was performed using ZFITTER [12]. In the fit the cross section and forward-backward asymmetry were calculated in terms of M_Z and Γ_Z and the vector and axial-vector coupling constants of the electron and muon. At tree level in the Standard Model, the relationships between these couplings and the forward-backward asymmetry and leptonic partial width are

$$\Gamma_\ell = \frac{G_F M_Z^{\,3}}{6\sqrt{2}\pi}(V_\ell^{\,2} + A_\ell^{\,2})$$

$$A_{FB}^{peak} = 3\left(\frac{V_e A_e}{V_e^{\,2} + A_e^{\,2}}\right)\left(\frac{V_\mu A_\mu}{V_\mu^{\,2} + A_\mu^{\,2}}\right)$$

with

$$V_e, V_\mu = -1/2 + 2\sin^2\theta_W,$$
$$A_e, A_\mu = -1/2,$$

where θ_W is the weak mixing angle. Higher order electroweak corrections modify the values of V_e,V_μ,A_e and A_μ, whilst essentially preserving the tree-level relations for the asymmetry and partial widths. These corrections are included in the calculations of reference [12]. The result of the fit is

$$V_e V_\mu = 0.0024 \pm 0.0015(\text{stat}) \pm 0.0004(\text{syst}),$$
$$A_e A_\mu = 0.253 \pm 0.003(\text{stat}) \pm 0.003(\text{syst})$$

with a χ^2/degree of freedom of 12.5/(14-2), and where the systematic errors include the effect of the uncertainty on the measurement of Γ_Z and M_Z. If we take the sign of these couplings to be negative, as determined by other experiments [13], then we obtain

$$V_\ell = -(V_e V_\mu)^{1/2} = -0.048\,^{+0.019}_{-0.014}(\text{stat}) \pm 0.004(\text{syst}),$$
$$A_\ell = -(A_e A_\mu)^{1/2} = -0.503 \pm 0.003(\text{stat}) \pm 0.003(\text{syst})$$

Fig.3 shows this result and the contours for the 70% and 95% confidence levels, in the V_ℓ,A_ℓ plane, along with the predictions of the Minimal Standard Model, assuming lepton universality and for a range of values of the top quark and Higgs masses. It can be seen that the data are in good agreement with the model.

5. Summary and Conclusions

The square root of the product of the Z° to e^+e^- and $\mu^+\mu^-$ leptonic partial widths has been determined to be

$$(\Gamma_e\Gamma_\mu)^{1/2} = 85.0 \pm 0.9(\text{stat}) \pm 0.8(\text{syst}) \text{ MeV}.$$

From this measurement of the partial width, the value of the effective weak mixing angle is determined to be

$$\sin^2(\overline{\theta_W}) = 0.2267 \pm 0.0037.$$

The ratio of the hadronic and muon pair partial widths is

$$\frac{\Gamma_h}{\Gamma_\mu} = 19.89 \pm 0.40(\text{stat}) \pm 0.19(\text{syst}).$$

The forward-backward asymmetry at $E_{cms} = 91.22$ GeV is found to be

$$A_{FB}^{peak} = 0.028 \pm 0.020(\text{stat}) \pm 0.005(\text{syst}).$$

A fit to $\sigma_{\mu\mu}$ and A_{FB} gives the following values for the product of the electron and muon vector and axial-vector coupling constants

$$V_eV_\mu = 0.0024 \pm 0.0015(\text{stat}) \pm 0.0004(\text{syst}),$$
$$A_eA_\mu = 0.253 \pm 0.003(\text{stat}) \pm 0.003(\text{syst}).$$

The results of this analysis are in agreement with the expectations of the Minimal Standard Model.

Acknowledgements

We are greatly indebted to our technical staff and collaborators and funding agencies for their support in building the DELPHI detector, and to members of the SL Division for the speedy commissioning and excellent performance of the LEP collider.

References

[1] CERN 89–08 Vol.1 (1989) p89 and p203, *Z* Physics at LEP1, edited by G. Altarelli, R. Kleiss and C. Verzegnassi.

[2] D. Yu Bardin *et al.*, *Z. Phys.* **C44** (1989) 493.
M.S. Bilenky and A.A. Sazonov, JINR preprint E2–89–792 (Dubna 1989).

[3] DELPHI Collaboration, P. Aarnio *et al.*, *Phys. Lett.* **B241** (1990) 425.

[4] ALEPH Collaboration, D. Decamp *et al.*, *Phys. Lett.* **B235** (1990) 399, and preprint CERN/PPE 90-104 (1990).
L3 Collaboration, B. Adeva *et al.*, *Phys. Lett.* **B238** (1990) 122, and *Phys. Lett.* **B250** (1990) 183, and preprint L3 #028 (1991).
MARK II Collaboration, G.S. Abrams *et al.*, *Phys. Rev. Lett.* **63** (1989) 2173.
OPAL Collaboration, M.Z. Akrawy *et al.*, *Phys. Lett.* **B240** (1990) 497, and *Phys. Lett.* **B247** (1990) 58.

[5] V.Hatton *et al.*, LEP Absolute Energy in 1990, LEP performance note 12 (1990), unpublished.

[6] DELPHI Collaboration, P.Aarnio *et al.*, The DELPHI detector at LEP, CERN-PPE/90-128.

[7] J.E. Campagne and R. Zitoun, *Z. Phys.* **C43** (1989) 469 and Proceedings of the Brighton Workshop on Radiative Corrections, Sussex, July 1989.

[8] DELPHI Event Generation and Detector Simulation — Users Guide, DELPHI Note 89–67 (1989), unpublished.

[9] S. Jadach and J. Was, *Comp. Phys. Com.* **36** (1985) 191.
S. Jadach *et al.*, CERN 89–08, vol.3 (1989) 67.

[10] DELPHI note 90–35, Monte Carlo event generator for two-photon physics; unpublished.

[11] DELPHI Collaboration, P. Abreu *et al.*, *Phys. Lett.* **B241** (1990) 435 and DELPHI Note 90-62, paper submitted to the Aspen Conference, January 1991 and paper in preparation.

[12] D. Yu Bardin *et al.*, DELPHI Note 89-71 (1989), unpublished.

[13] See for example G.Altarelli, Proceedings of the 1989 International Symposium on Lepton and Photon Interactions at High Energies, Stanford University, August 7-12 (1989) 286.

[14] DELPHI Collaboration, P. Abreu *et al.*, *Phys. Lett.* **B247** (1990) 167 and *Phys. Lett.* **B252** (1990) 149.

Table 1. The number of selected events and cross sections $\sigma_{\mu\mu}$ for $e^+e^- \rightarrow \mu^+\mu^-$ for different centre of mass energies. The cross sections are corrected for the cuts on momenta and acollinearity angles and to the full solid angle. The errors are statistical only. The overall systematic error on these points is 0.8% on the total number of $\mu^+\mu^-$ events and 0.9% on the luminosity, including the estimated theoretical uncertainty on the luminosity. This gives a total sytematic error of 1.2% on the cross sections.

$\sqrt{s}$ (GeV)	No. of $\mu^+\mu^-$ events	$\sigma_{\mu\mu}$ (nb)
88.22	30	0.229 ± 0.042
89.22	81	0.420 ± 0.047
90.22	203	1.119 ± 0.078
91.22	1795	1.560 ± 0.037
92.22	194	1.206 ± 0.086
93.22	90	0.587 ± 0.062
94.22	82	0.389 ± 0.043

Table 2. Results of measurements of the forward-backward asymmetry A_{FB} for different centre of mass energies. The results are corrected to the full solid angle, but not for the cuts on momenta and acollinearity. The errors are statistical only. The overall systematic error on these points is ± 0.005.

$\sqrt{s}$ (GeV)	A_{FB}
88.22	-0.15 ± 0.13
89.22	-0.26 ± 0.10
90.22	-0.08 ± 0.06
91.22	0.028 ± 0.020
92.22	0.00 ± 0.06
93.22	0.10 ± 0.08
94.22	0.20 ± 0.09

Figure Captions

Fig.1. The distribution of the electric charge multiplied by the inverse momentum for reconstructed tracks in the polar angle range $22° < \theta < 158°$ and used in the $e^+e^- \to \mu^+\mu^-$ analysis of the forward-backward asymmetry.

Fig.2. a) Cross sections and b) forward-backward asymmetries for $e^+e^- \to \mu^+\mu^-$ as a function of the centre of mass energy around the Z° pole. The cross sections and asymmetries are corrected to full 4π angular acceptance. The errors shown are statistical only. The curves are the results of fits to the data as described in the text.

Fig.3. Measured values of V_ℓ and A_ℓ, together with contour plots for the 70% and 95% confidence levels. Also shown are the predictions of the Minimal Standard Model for a range of values of the top quark mass (as shown) and for a Higgs mass in the range 40 to 1000 GeV, which gives rise to the width of the band shown.

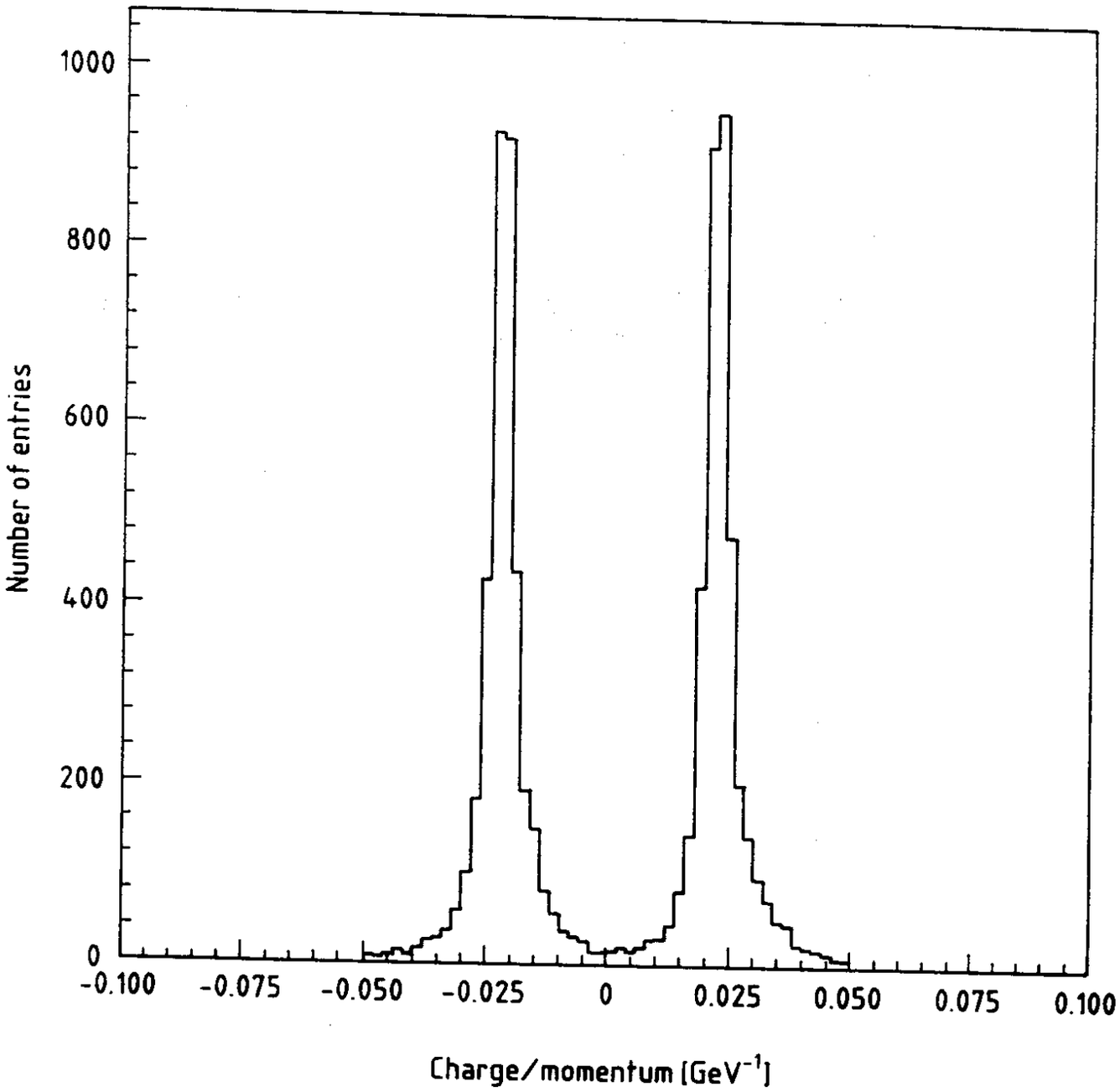
1000
800
600
400
200
0
Number of entries
-0.100
-0.075
-0.050
-0.025
0
0.025
0.050
0.075
0.100
Charge/momentum [GeV^{-1}]

Fig. 1

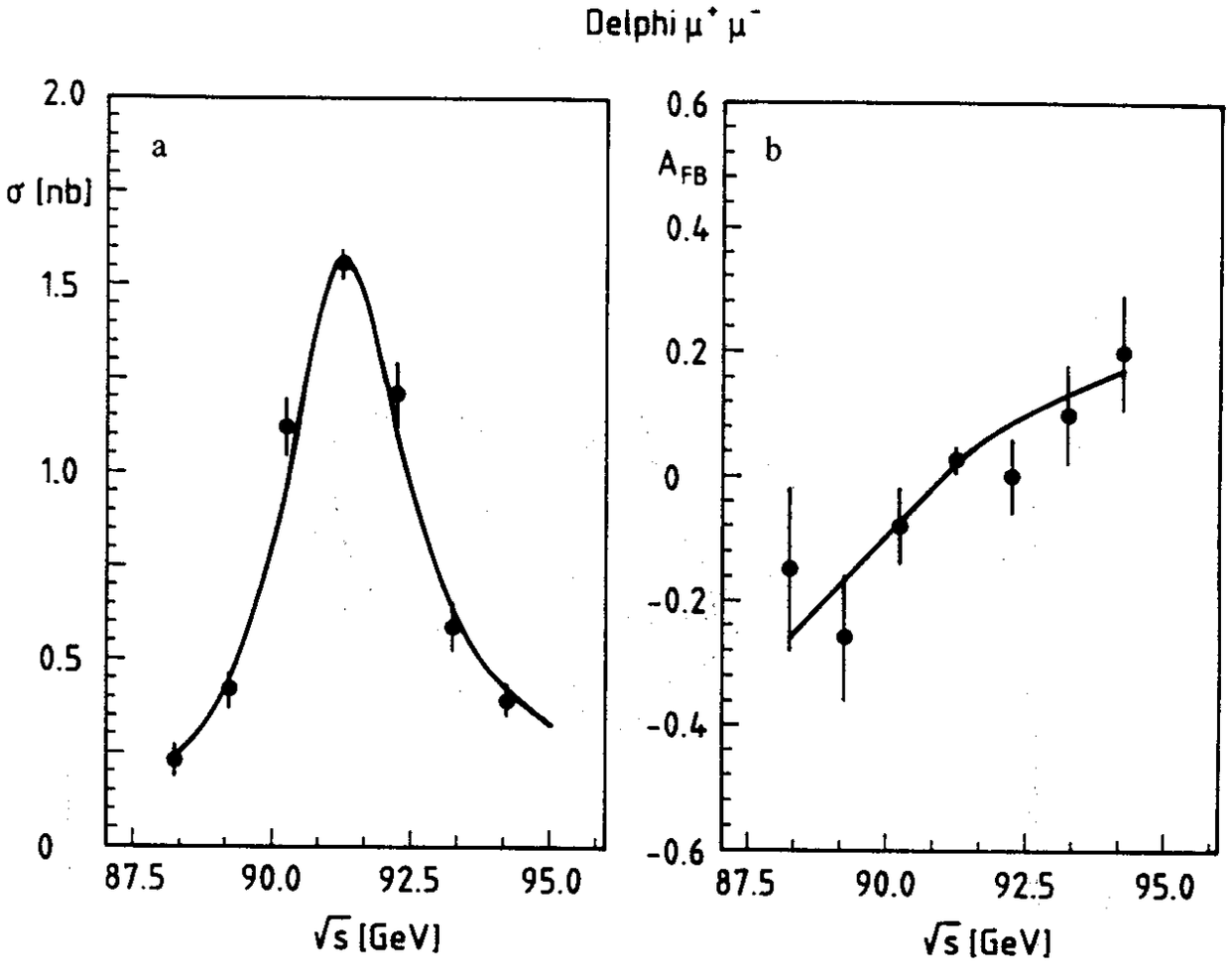
Delphi μ⁺ μ⁻
a
σ [nb]
2.0
1.5
1.0
0.5
0
87.5
90.0
92.5
95.0
√s [GeV]
b
A_FB
0.6
0.4
0.2
0
-0.2
-0.4
-0.6
87.5
90.0
92.5
95.0
√s [GeV]

Fig. 2

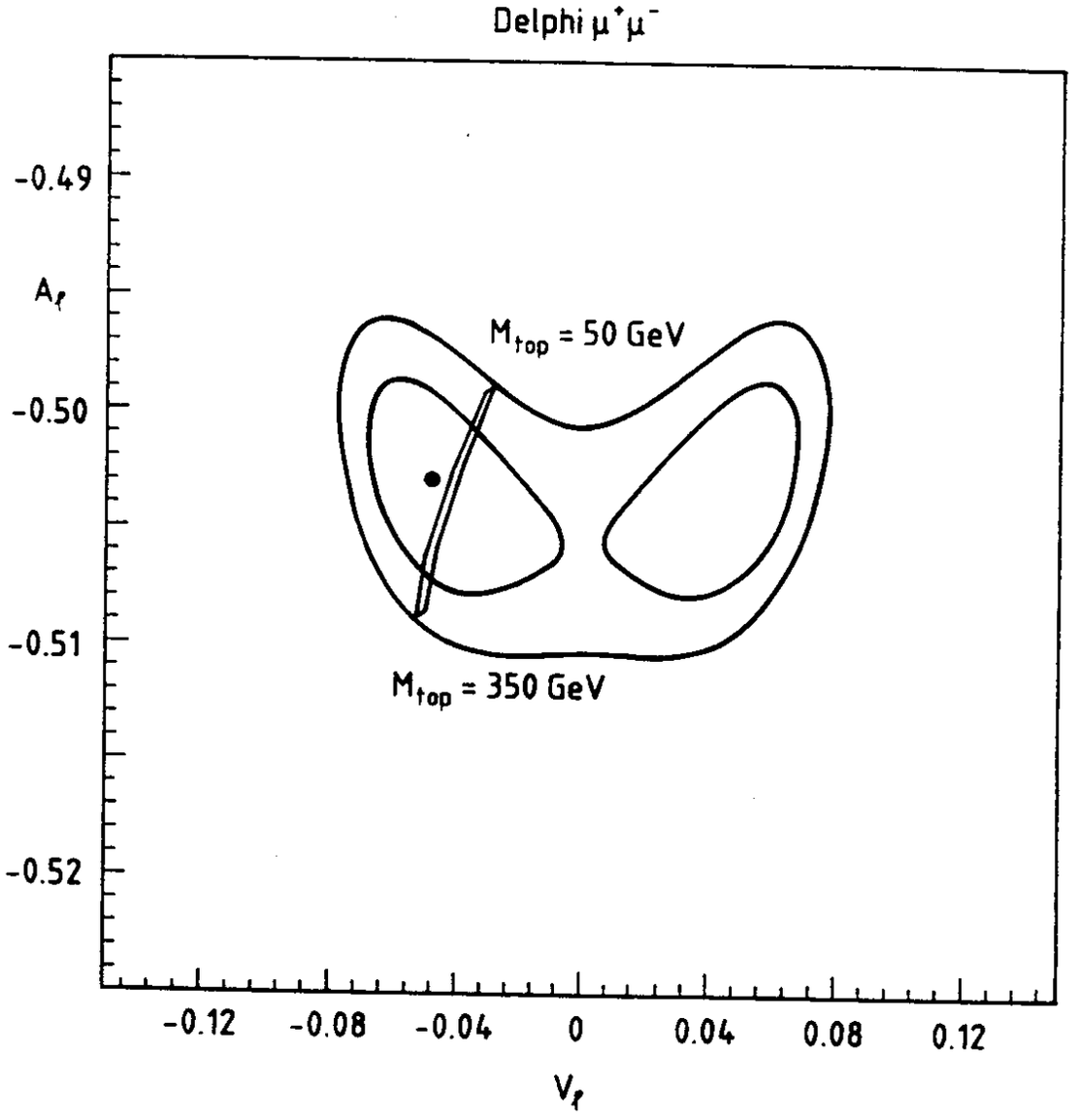
Delphi μ⁺μ⁻
-0.49
A_f
-0.50
-0.51
-0.52
M_{top} = 50 GeV
M_{top} = 350 GeV
-0.12
-0.08
-0.04
0
0.04
0.08
0.12
V_f

Fig. 3